Implant Design and Cervical Spinal Biomechanics and Neurorehabilitation: A Finite Element Investigation

Hossein Bahreinizad, MS; Suman K. Chowdhury, PhD

ABSTRACT

Introduction:

The cervical spine, pivotal for mobility and overall body function, can be affected by cervical spondylosis, a major contributor to neural disorders. Prevalent in both general and military populations, especially among pilots, cervical spondylosis induces pain and limits spinal capabilities. Anterior Cervical Discectomy and Fusion (ACDF) surgery, proposed by Cloward in the 1950s, is a promising solution for restoring natural cervical curvature. The study objective was to investigate the impacts of ACDF implant design on postsurgical cervical biomechanics and neurorehabilitation outcomes by utilizing a biofield head-neck finite element (FE) platform that can facilitate scenario-specific perturbations of neck muscle activations. This study addresses the critical need to enhance computational models, specifically FE modeling, for ACDF implant design.

Materials and Methods:

We utilized a validated head-neck FE model to investigate spine–implant biomechanical interactions. An S-shaped dynamic cage incorporating titanium (Ti) and polyetheretherketone (PEEK) materials was modeled at the C4/C5 level. The loading conditions were carefully designed to mimic helmet-to-helmet impact in American football, providing a realistic and challenging scenario. The analysis included intervertebral joint motion, disk pressure, and implant von Mises stress.

Results:

The PEEK implant demonstrated an increased motion in flexion and lateral bending at the contiguous spinal (C4/C5) level. In flexion, the Ti implant showed a modest 5% difference under 0% activation conditions, while PEEK exhibited a more substantial 14% difference. In bending, PEEK showed a 24% difference under 0% activation conditions, contrasting with Ti's 17%. The inclusion of the head resulted in an average increase of 18% in neck angle and 14% in C4/C5 angle. Disk pressure was influenced by implant material, muscle activation level, and the presence of the head. Polyetheretherketone exhibited lower stress values at all intervertebral disc levels, with a significant effect at the C6/C7 levels. Muscle activation level significantly influenced disk stress at all levels, with higher activation yielding higher stress. Titanium implant consistently showed higher disk stress values than PEEK, with an orders-of-magnitude difference in von Mises stress. Excluding the head significantly affected disk and implant stress, emphasizing its importance in accurate implant performance simulation.

Conclusions:

This study emphasized the use of a biofidelic head-neck model to assess ACDF implant designs. Our results indicated that including neck muscles and head structures improves biomechanical outcome measures. Furthermore, unlike Ti implants, our findings showed that PEEK implants maintain neck motion at the affected level and reduce disk stresses. Practitioners can use this information to enhance postsurgery outcomes and reduce the likelihood of secondary surgeries. Therefore, this study makes an important contribution to computational biomechanics and implant design domains by advancing computational modeling and theoretical knowledge on ACDF–spine interaction dynamics.

Cervical spondylosis, a common musculoskeletal disorder of the cervical spine, is prevalent in both general population (affecting over 50% of middle-aged individuals[1,2]) and military personnel (especially among pilots[3,4]). It is also a leading cause of neural disorders in the cervical spine,[5,6] inducing pain and limiting the movement of the spine, thus significantly diminishing the quality of life for those affected. When nonsurgical treatments prove to be ineffective in relieving symptoms of cervical spondylosis, surgery becomes a viable option. Anterior Cervical Discectomy and Fusion (ACDF) surgical method, initially proposed by Smith and Robinson[7] and improved by Cloward in the 1950s,[8] offers a compelling solution by providing effective decompression and restoring the natural curvature of the cervical spine. Anterior Cervical Discectomy and Fusion stands out as the gold standard in anterior cervical approaches for a range of other cervical spinal

Department of Industrial, Manufacturing, and Systems Engineering, Texas Tech University, Lubbock, TX 79409-3061, USA

Preliminary results were presented at the Military Health System Research Symposium, which was held in August 2023.

Corresponding author: Suman K. Chowdhury, PhD, USA (suman.chowdhury@ttu.edu).

doi:https://doi.org/10.1093/milmed/usae279

injuries and disease conditions, including herniated discs, cervical stenosis, and other degenerative disk diseases. Especially, the fusion surgery involving the placement of implants and bone grafting facilitates cervical realignment and tackles potential spinal cord injuries by alleviating nerve pressure and improving neck stability.[9,10] Between 2006 and 2013, an annual average of 137,000 ACDF surgeries were performed in the United States alone.[11]

Although ACDF surgery stands out as an effective solution for cervical spondylosis, patients who have undergone this procedure often need a second surgical intervention because of adjacent segment degeneration. Depending on the specific affected levels, this degeneration can manifest in superior, inferior, or adjacent levels. Earlier studies have linked this complication to abnormal kinematics caused by fusion (the placement of an implant) and increased disk pressure at the adjacent level.[12] Furthermore, the impact of ACDF on the short- and long-term quality of life for individuals undergoing the surgery raises concerns. A study on U.S. Navy personnel revealed an 88% return to active flying post-ACDF, with an average duration of 15.2 weeks for full duty resumption.[13] These findings underscore the importance of effective cervical implant design for enhanced biomechanical and neurorehabilitative outcomes after ACDF surgery. However, assessing the biomechanical response of the cervical implant and its adjacent cervical intervertebral joints postsurgery poses challenges, especially in reliably measuring internal stress in disks through both in vivo and in vitro methods.

Previous studies[14–17] showed that the design and material properties of cervical ACDF implants affect postsurgical kinematics and neurorehabilitation. The design of these implants has evolved with the help of finite element (FE)–based computational models. These FE-based spinal models have been employed to explore valuable insights into the ACDF implants and cervical spinal mechanisms.[14–16] However, for a comprehensive understanding of the spine–implant dynamics, it is essential to incorporate a biofidelic head-neck computational model.[9] In various fields such as medicine, automotive safety testing, and biomechanics, the biofidelity of a computational model—the degree to which a model accurately represents the biological system—is crucial for ensuring that simulations closely resemble real-world conditions or experimental results. A poorly defined computational model can lead to misleading results, highlighting the importance of detailed and accurate representation of different parts of the model in such simulations. In the case of evaluating the ACDF implant, most studies used FE models consisting of contiguous cervical vertebrae[18] without considering the roles of neck muscles and the head structures that primarily control cervical spinal stabilization and mobility. For instance, Manickman et al.[18] utilized a cervical vertebrae model consisting of cervical vertebrae C3/C6 without active muscles to assess an S-shaped cervical implant. Sun et al.[15] focused on topology optimization for the design of the cervical impact cage using a cervical vertebrae model (C2/C5) without neck muscles. Similarly, Liu et al.[19] explored using memory compression alloys in cervical implant design with a cervical vertebrae model (C3/C7) lacking active muscles. Moussa et al.[2] concentrated their study on a model limited to C6 and C7, excluding neck muscles, to assess how an optimized porous material structure performs in mitigating the risk of subsidence. Additionally, Lin et al.[20] investigated the impact of cage screws on the biomechanical characteristics of the human spine, implanted cage, and associated hardware using a cervical vertebrae model (C3/C5) without active muscles. In a separate study, Lin et al.[16] extended their research to a cervical vertebrae model (C2/C6) without active muscles, examining the effects of biomechanical strength and increased contact area on the mechanical response of cervical vertebrae and implants. Furthermore, Kwon et al.[21] conducted a comparative study on the biomechanical effects of plates with varying lengths and different screw insertion angles, employing a cervical vertebrae model (C3/C6), omitting neck muscles. Despite significant advancements in head-neck FE models and, specifically, cervical vertebrae models,[22,23] those used in ACDF studies often lack crucial details, such as active muscles. Since it has been demonstrated[22–24] that active muscles influence the biomechanical response of the neck, omitting them leads to misleading results. Additionally, in real-world scenarios, the head structures, even when considered as a mass with specific inertial properties, impact the mechanical response of the neck. Consequently, it should be noted that experimental models[25] of neck mechanics commonly include a surrogate head to simulate the inertia properties of the head.

Utilizing these models offers valuable insights into various facets of ACDF implant design, particularly in guiding the selection of materials. The integration of artificial cages, incorporating materials like stainless steel, titanium (Ti), carbon fiber, polymethyl methacrylate, and polyetheretherketone (PEEK), into cervical spine procedures has significantly advanced ACDF. Polyetheretherketone emerges as the primary choice, with 46% of patients opting for PEEK implants, followed by 31% with Ti cages, 18% with cage–screw combinations, and 5% with Polymethyl methacrylate cages.[26] Additionally, various numerical[18,27] and experimental[28,29] studies have found favorable results for PEEK material owing to its lower subsidence rates and capacity to provide the neck with a higher range of motion. Nevertheless, each material choice for implants in ACDF procedures presents unique pros and cons. For instance, Ti and its alloys are known for their biocompatibility, high stiffness, corrosion resistance, and low density.[28] Additionally, the inherent rigidity of Ti provides the cervical spine with good stability post-ACDF surgery. In contrast, PEEK's lower stiffness allows increased neck flexibility and a potentially lower subsidence rate,[27,28] albeit with concerns of prolonged fusion times[30] than Ti. Furthermore, several FE studies have conducted side-by-side comparisons between PEEK and Ti implants. For instance, Qi et al.[27] reported that utilizing PEEK as the material for both endplates and the

mobile insert resulted in a smaller overall mean of the absolute values of percentage change in principal intersegmental motions compared to Ti. Additionally, in separate studies, Manickam et al.[18,31] observed that PEEK implants showed greater range of motion at the fusion level and adjacent levels while experiencing lower stress within the cage when compared to Ti. However, the aforementioned FE studies did not investigate how the material properties of these ACDF mentioned earlier implants affect neck biomechanics and neurorehabilitation by using a biofidelic computational model, which includes a detailed head-neck system and considers neck muscle activation strategies.

Therefore, this study aimed to investigate the effects of ACDF implant design using two materials—Ti and PEEK—on postsurgical cervical spinal biomechanics and neurorehabilitation outcomes by leveraging a biofidelic head-neck FE model. We also numerically explored the implant and cervical spinal interaction for a simulated post-ACDF surgery scenario by perturbing various neck muscle activation strategies with and without the presence of head structures. In this study, the assessment of cervical intervertebral kinematics was considered the core determinant of neck neurorehabilitation outcomes. At the same time, the biomechanical outcomes include the analysis of von Mises stress on implants and individual cervical intervertebral discs.

METHODS

FE Model

We utilized our previously validated head-neck FE modeling platform,[32] developed from detailed magnetic resonance imaging (MRI) data, to explore spine–implant biomechanical interactions (Fig. 1A). This comprehensive model includes the scalp, skull, cerebrospinal fluid (CSF), brain, dura mater, pia mater, cervical vertebrae (C1-C7), intervertebral discs, 14 ligaments (anterior longitudinal ligament, posterior longitudinal ligament, ligamentum flavum, capsular ligament, interspinous ligaments, tectorial membrane, anterior and posterior atlanto-occipital ligaments, anterior and posterior atlanto-axial ligaments, apical ligament, alars ligament, transverse ligament, and cruciate ligament of atlas), and 42 neck muscles (obliquus capitis superior, superior longus colli, rectus capitus major, rectus capitus minor, longus capitis, rectus capitis ant, rectus capitis lat, anterior scalene, middle scalene, posterior scalene, sternocleidomastoid, longissimus capitis, longissimus cervicis, multifidus cervicis, semisplenius capitus, semispinalis cervicis, splenius capitis, splenius cervicis, levator scapula, oblique capitus inferior, and trapezius), all constructed from 42-year-old male firefighter MRI data (height: 176 cm, weight: 106 kg) and totaling 1.36 million elements. The subject's body mass index (BMI) was calculated to be 34.2, and their BMI-based body fat percentage was estimated to be 34.5%.[33] To capture the intricacies of the cervical vertebrae (C1–C7) and intervertebral discs, we used 72,000 second-order tetrahedral elements. A linear elastic model represented vertebral mechanical behavior, while the complex mechanical behavior of intervertebral discs was described using a hyper-viscoelastic material model. Additionally, neck ligaments were modeled as linear springs. Furthermore, the scalp and skull included 0.27 million and 0.23 million tetrahedral elements, respectively. Quad shell elements totaled 0.1 million, with the dura and pia maters accounting for 0.05

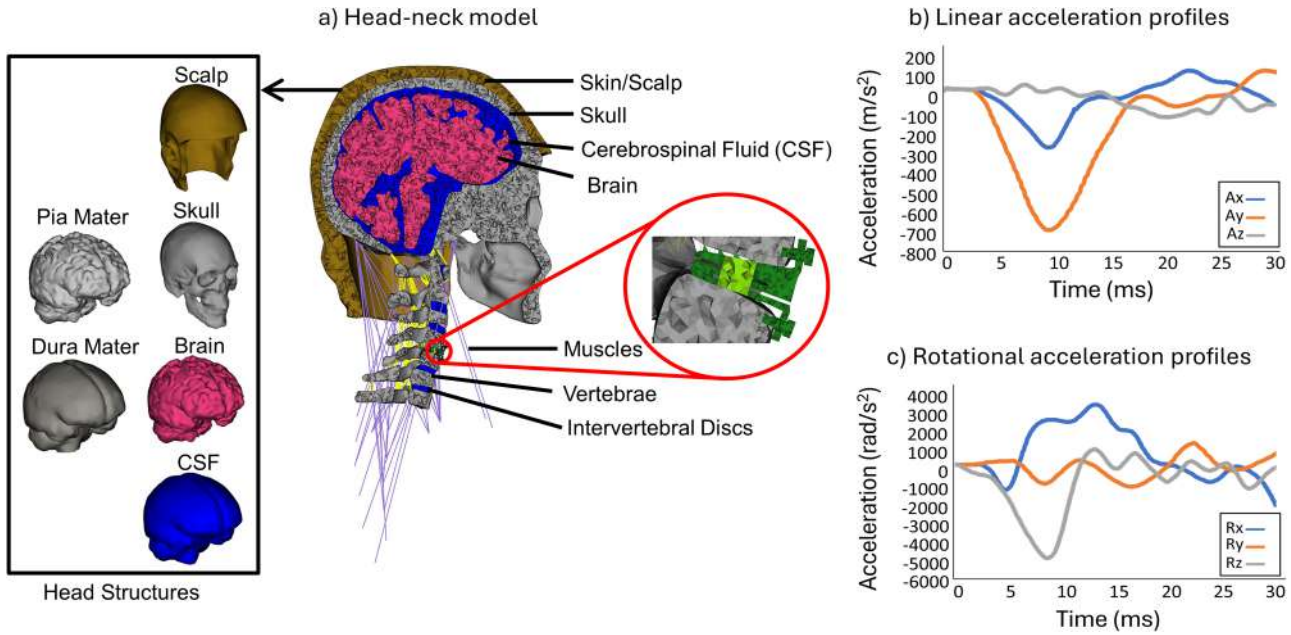

FIGURE 1. (A) A schematic representation of the head-neck FE model that includes scalp, skull, brain, pia and dura mater, CSF, cervical vertebrae, intervertebral discs, 14 ligaments, and 42 active muscles. The load condition included 6 experimental head-neck acceleration profiles[35] commonly seen in helmet-to-helmet collisions in American football: (B) 3 linear acceleration (Ax, Ay, and Az) and (C) 3 rotational acceleration (Rx, Ry, and Rz).

million and 0.04 million elements, respectively. The skull, pia mater, and dura mater were characterized as linear elastic material. The scalp was modeled using a linear viscoelastic material, CSF as a hyperelastic material, and the brain's gray and white matter as a hyper-viscoelastic material. A distinctive feature of our model is the incorporation of the hill-type muscle model, allowing for the simulation of active muscle behavior and providing insights into the impact of muscle activation on neck biomechanics.

Implant Model

The implant design used in this study included an S-shaped dynamic cage with 2-screw fixation and a rectangular bone graft. The chosen cage design, derived from the literature,[18] possesses unique features. Its trapezoidal shape optimizes vertebral body contact, while the wedge-shaped structure maintains natural cervical lordosis and intervertebral disc height. Surface teeth prevent migration, and the zero-profile design with a two-screw fixation system, ensures stability while minimizing adjacent segment stress. We reconstructed this implant using SolidWorks software (Dassault Systems, France) by meshing it with 42,000 tetrahedral elements in the ANSA (BETA CAE Systems SA, Greece) platform. The implant was then positioned at the C4/C5 level by replacing the intervertebral disc—the model's C4/C5 disk was modified for the cage placement and fixing it with anterior plates and screws. To describe its mechanical response, we used a linear elastic model.

This study tested 2 different implant materials—Ti and PEEK—and conducted several computational simulations of spine–implant interaction at the C4/C5 level. We adopted material properties for these 2 materials from the literature,[15,18,34] including Young's modulus of 110 GPa and 3.6 GPa, Poisson's ratios of 0.3 and 0.3, and densities of 4429 kg/m^3 and 1300 kg/m^3 for Ti and PEEK materials, respectively. To define the contacts, we applied a tied contact between the implant and its adjunct vertebrae (C4 and C5) and a constraint to prevent self-penetration.

Loading Condition and Study Design

The selection of head-neck kinematic profiles is essential to evaluate the postsurgical kinematic response of the head-neck system and the implant–disk stress distribution. Instead of normal head-neck kinematic patterns, in this study, we considered injury-prone head-neck kinematic patterns. Such scenarios would provide unprecedented knowledge about the durability and mechanical response of the implant material and the biomechanical response of the spine–implant interaction site. Therefore, we selected both linear (Ax, Ay, and Az) and rotational (Rx, Ry, and Rz) accelerations of the head-neck system commonly seen in helmet-to-helmet concussive impact scenarios.[35] By using dummies, the study by Zhang et al.[35] replicated American football players' helmet-to-helmet collisions and recorded resulting head acceleration profiles. We adopted these acceleration profiles as the loading condition in this study (Fig. 1B and C). Although our simulation was based on American football collisions, the combined linear and rotational acceleration exceeding 7g is relevant for military contexts. For instance, jet pilots commonly experience high combined linear and rotational acceleration, with Gz acceleration reaching up to 9g or more.[36] We applied these acceleration profiles to FE models with and without implants (Fig. 1B and C). The acceleration profiles were applied to the head center of gravity in models with heads and to the top of the cervical vertebrae (C1) in models without the head.

The without-implant condition simulated intact or normal disks. In contrast, with-implant conditions represented scenarios with inserted implants. These models incorporated three muscle activation patterns (0%, 25%, and 80% activation levels) across all muscles. Nonetheless, the individual muscle force varied over simulation duration because of the changes in the muscle length and muscle velocity. Additionally, we performed simulations with and without the presence of the head to assess its impact on the biomechanical response of the neck. This approach realistically allows us to simulate the postsurgery performance of the neck and implant.

We calculated flexion angle (°), lateral bending angle (°), and disk pressure (MPa) of all cervical intervertebral joints, in addition to the implant von Mises stress (MPa) in META software (BETA CAE Systems SA, Greece). The flexion angle was quantified by evaluating the degree of anterior movement of vertebrae in the sagittal plane. In contrast, the lateral bending angle was assessed by calculating the degree of lateral deviation of vertebrae in the frontal plane. Intervertebral flexion and lateral bending motion (°) were determined as the angular difference between the minimum and maximum angles of a specific vertebrae with respect to its adjacent vertebrae. The total motion of the neck was defined as the cumulative sum of the total motion of individual cervical vertebral joints.

Statistical Data Analysis

We used Analysis of Variance (ANOVA) to assess the impact of our independent variables (implant type, muscle activation level, and the presence of the head) on the dependent variable (disk pressure) with a 95% confidence level ($\alpha = .05$). As our head-neck FE model implied the same muscle activation throughout the simulation time, we conducted the ANOVA by treating the time effect as a randomized block. The randomized block ANOVA allowed us to examine how the independent variables individually and collectively (interaction effect) affected the individual disk pressure over the course of the simulation duration. We performed 10 ANOVA tests in total: eight for intervertebral disc stress and two for implant stress. All statistical analyses were conducted using R software version 4.2.3.

RESULTS

In the analysis of C4/C5 motion, PEEK consistently exhibited higher angles than Ti, both with and without the presence

TABLE I. The Angular (°) Responses of the Whole Neck and C4/C5 (Contiguous Level) Under Various Spine–Implant Interaction Simulations With the Presence of the Head

		Neck		C4/C5	
Muscle activation	**Implant type**	**Flexion (°)**	**Lateral bending (°)**	**Flexion (°)**	**Lateral bending (°)**
No activation	No implant	63.61	34.23	19.99	7.48
	PEEK	57.96 (−8.88%)	28.12 (−17.85%)	18.65 (−6.70%)	10.21 (+36.50%)
	Ti	61.76 (−2.91%)	33.82 (−1.20%)	16.33 (−18.31%)	8.26 (+10.43%)
25% activation	No implant	65.22	33.63	20.48	6.84
	PEEK	64.53 (−1.06%)	29.99 (−10.82%)	18.22 (−11.04%)	9.78 (+3.22%)
	Ti	65.78 (+0.86%)	32.32 (−3.90%)	16.62 (−18.85%)	7.06 (+3.22%)
80% activation	No implant	73.76	33.66	20.7	9.69
	PEEK	69.18 (−6.21%)	34.99 (+3.95%)	17.49 (−15.51%)	10.6 (+9.39%)
	Ti	69.02 (−6.43%)	36.77 (+9.24%)	16.8 (−18.84%)	7.46 (−23.01%)

Percent changes from the baseline (no implant) are shown in parentheses alongside the respective angular values.

TABLE II. The Angular (°) Responses of the Whole Neck and C4/C5 (Contiguous Level) Under Various Spine–Implant Interaction Simulations Without the Presence of the Head

		Neck		C4/C5	
Muscle activation	**Implant type**	**Flexion (°)**	**Lateral bending (°)**	**Flexion (°)**	**Lateral bending (°)**
No activation	No implant	55.69	32.63	16.81	7.07
	PEEK	45.92 (−17.54%)	23.64 (−27.55%)	14.89 (−11.42%)	9.67 (+36.78%)
	Ti	54.35 (−2.41%)	32.56 (−0.21%)	11.91 (−29.15%)	8.54 (+20.79%)
25% activation	No implant	56.88	31.72	17.61	5.73
	PEEK	54.34 (−4.47%)	29.64 (−6.56%)	15.58 (−11.53%)	8.3 (+44.85%)
	Ti	54.71 (−3.82%)	30.8 (−2.90%)	11.92 (−32.31%)	6.48 (+13.09%)
80% activation	No implant	64.29	32.67	17.48	7.46
	PEEK	60.37 (−6.10%)	33.37 (2.14%)	15.63 (−10.58%)	10.08 (+35.12%)
	Ti	61.34 (−4.59%)	34.42 (5.36%)	14.87 (−14.93%)	7.7 (+3.22%)

Percent changes from the baseline (no implant) are shown in parentheses alongside the respective angular values.

of the head. Furthermore, the PEEK implant showed the highest lateral bending angles, whereas no implant condition exhibited the highest flexion angles across all muscle activation levels (Tables I and II). In the examination of whole neck motion, the Ti implant showed greater flexion and lateral bending angles than the PEEK implant, both with and without the presence of the head, except for 80% activation flexion with the presence of the head. Additionally, our results showed that no implant surpassed the Ti implant in flexion and lateral bending angles with and without the presence of the head, except for 80% activation lateral bending and 25% activation flexion angles. Exclusion of the head resulted in an average decrease of 10% in neck angle and 13% in C4/C5 angle across all three implant conditions and muscle activation levels. Additionally, the whole neck flexion angle increased by an average of 9% at 80% activation compared to no activation (Tables I and II).

The stress analysis data consistently showed a lower value for the PEEK implant at all intervertebral disc levels than the Ti implant (Fig. 2A and B). The addition of head structures to the model showed comparatively lower differences in stress values between the PEEK and Ti implants, with ∼10.48% (for no activation), ∼5.90% (for 25% activation), and ∼1.23% (for 80% activation) lower for PEEK implant design than the Ti implant design. In contrast, without head structures, the neck-only model showed ∼15.12% (nor No activation), ∼6.45% (for 25% activation), and ∼3.58% (for 80% activation) lower stress values for PEEK compared to Ti. In addition, Fig. 2A and B show that adding head structures to the model yielded greater stress values across all disks and implant types than the model with neck-only structures. The implant material type was statistically significant only at C6/C7 levels ($P < .05$). Conversely, an increase in muscle activation level significantly increased intervertebral disc stress across all intervertebral levels ($P < .05$) (with head: ∼41.39% for No implant, ∼37.80% for PEEK, ∼32.92% for Ti; without head: ∼48.03% for No implant, ∼64.07% for PEEK, ∼60.36% for Ti).

The Ti implant consistently exhibited significantly higher implant stress values compared to the PEEK implant across all muscle activation levels ($P < .05$) (with head: ∼90.28% for No activation, ∼90.20% for 25% activation, ∼90.24% for 80% activation; without head: ∼82.63% for No activation, ∼83.99% for 25% activation, ∼81.03% for 80% activation) (Fig. 1D and E). Additionally, excluding the head also significantly decreased disk and implant stress ($P < .05$), emphasizing the head's importance in accurate implant performance simulation.

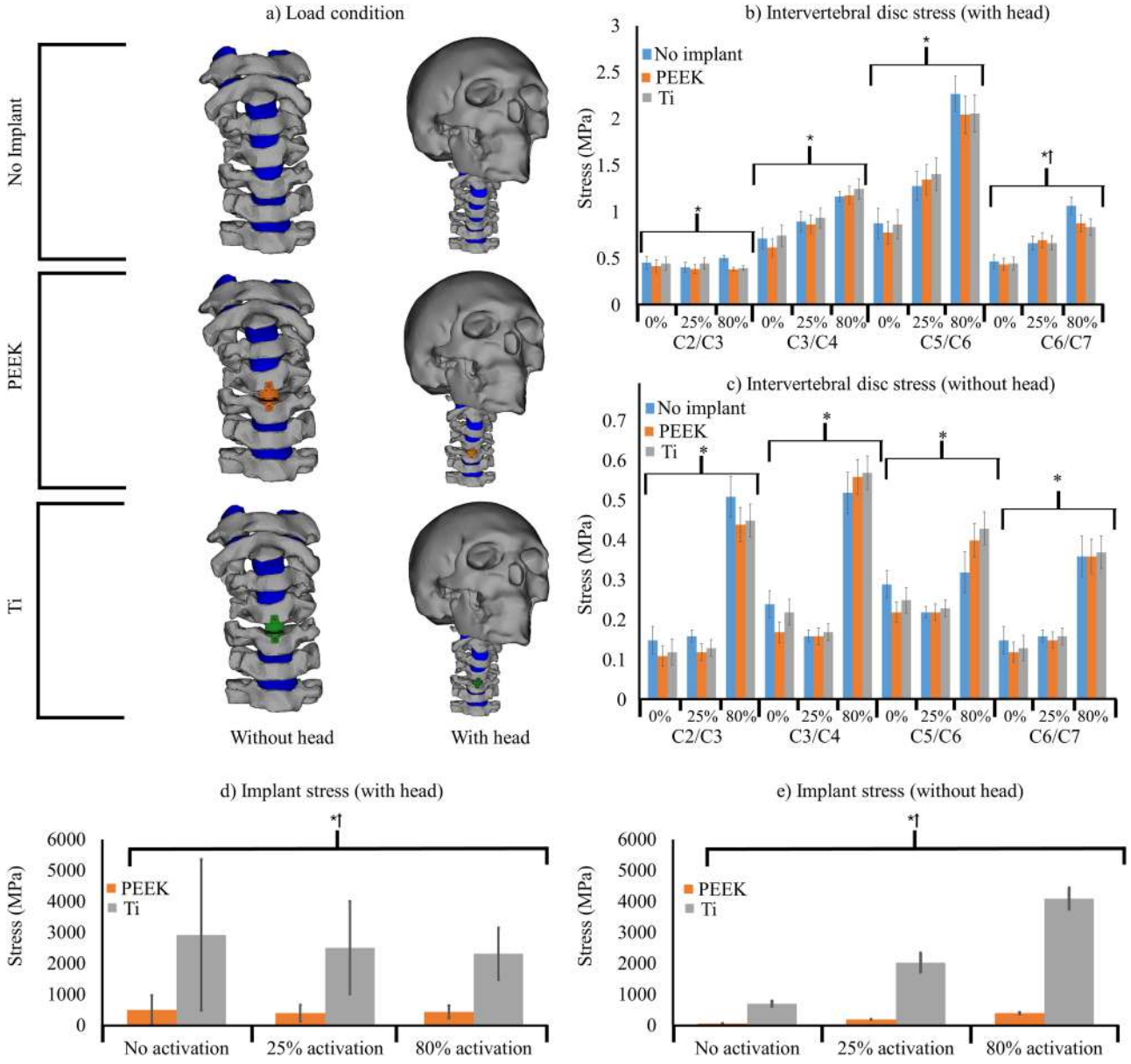

FIGURE 2. (A) A visual depiction of the load condition depicting the dynamic interplay between cervical vertebrae and implants with and without the presence of head structures. Muscle activation and implant type effects on the mean von Mises stress (mean and SE) of individual intervertebral discs for two modeling conditions: (B) With and (C) without the presence of the head structures. Similarly, the effects of muscle activation and implant type on the maximum von Mises stress of the implants under two modeling conditions: (D) With and (E) without the presence of the head. The asterisks (*) and (†) indicate the statistical significance of muscle activation and implant material, respectively.

DISCUSSION

This study had a two-fold objective: First, to improve the computational models for ACDF by investigating the influence of neck muscle activity and the presence of the head and second, to assess the differences between Ti and PEEK implant materials for enhanced postsurgery implant performance. By delving into these aspects, we sought to provide a more comprehensive understanding of the biomechanical complexities involved in ACDF procedures. This approach is crucial for refining computational models and optimizing implant design to positively impact postsurgery outcomes, reduce recovery times, and minimize the need for additional interventions in both civilian and military populations.

Anterior Cervical Discectomy and Fusion implants are used for a range of cervical spinal injuries and disease conditions, including herniated discs, cervical stenosis, and other degenerative disk diseases, in addition to cervical spondylolysis. Such cervical spinal injuries, such as current or past cervical spondylolysis, typically disqualify military personnel. Nonetheless, surgically treated cervical diseases may be waivable and allow military personnel to return to duty based on expert opinion.[37] The implications of ACDF implants in

rehabilitating such cervical disease among both military and civilian populations are pretty common. Although the effects and outcomes of these treatments have been studied in civilian and military populations, research on their use in the high-acceleration environments of military aviation is limited.[37] This highlights the importance of this study in evaluating the postsurgery performance of ACDF implants, particularly in high-acceleration scenarios.

Our findings revealed that the presence of the head significantly impacts both implant and neck biomechanical responses. The head's weight and inertial properties increased the forces and moments acting on the cervical disks, thereby imposing higher stress values on individual disks and implants. Although prior computational studies in the impact biomechanics domain emphasized on the inclusion of both head and neck structures for a holistic understanding of neck injury,[14,22,23,25] studies on ACDF implant designs using computational models have consistently overlooked the inclusion of head structures thus far.[2,15,16,18,20] Similarly, the inclusion of active neck muscles significantly affected the biomechanical response of the model. Neck muscles exert compressive force on the neck and head, providing stability and mobility. These forces transmit from the muscle insertion points to the intervertebral discs, resulting in stress and deformation of the disks. Consistent with previous numerical[22,24] and experimental[38] studies on neck biomechanics, which have considered neck muscles in their models, our results emphasized the effect of active neck muscles on ACDF implant design. Additionally, our findings aligned with the existing literature, indicating that neck muscle activity significantly influences neck kinematic response.[22,24,38]

Regarding material effects, we evaluated two widely used implant materials, PEEK and Ti. Our results align with prior studies,[18,31,39] reinforcing the notion that PEEK demonstrates a higher angle at the implant level than Ti. Compared to Ti, the lower stiffness of PEEK enables it to deform more efficiently, resulting in an increased angle at the implant level. Conversely, compensating for Ti's reduced flexibility, other intervertebral discs must deform more, contributing to increased neck motion. This phenomenon potentially explains the increased stress levels observed in cervical disks with Ti implants. Furthermore, ensuring material properties match those of surrounding tissue is critical to avoid adverse effects such as stress shielding.[28] In this regard, PEEK's stiffness of 3.6 GPa is more closely aligned with bone stiffness.[40] Compared to Ti, which has a stiffness of 110 GPa. This closer match provides a notable advantage for PEEK regarding material compatibility.

Our study had several limitations. The head-neck model of this study did not distinguish between cancellous and cortical regions in bone or between annulus fibrosus and nucleus pulposus in intervertebral discs. Also, we used only one loading condition, although it was based on real-life sports data. Exploring additional scenarios could enhance our understanding of the post-ACDF surgery performance of the neck and implant. Furthermore, our study assessed only one type of novel cage design, where different cage designs might influence the choice of materials. Additionally, our subjects had a high BMI, which may represent only a tiny subset of the military population. However, we assessed the morphological structures of the head and neck of the modeled subject in our previous studies.[32] Our findings indicated that the geometric dimensions, such as the scalp thickness, skull thickness, brain volume, CSF volume, cervical disk heights, and cervical vertebrae dimensions, fall within the range of a normal subject's morphological structures (a healthy BMI of 25). In this context, the modeled head and neck structures' morphological structures represent healthy civilian and military personnel's head-neck structures. Nonetheless, further investigations are required to generalize our findings by scaling the model structures representing various BMI groups. Finally, we selected only two implant materials. Future studies may consider assessing various other alternate materials and geometric properties.

CONCLUSIONS

This study evinced the importance of employing a biofidelic head-neck model in computational studies while assessing the effects of various ACDF implant designs on cervical spinal biomechanical and neurorehabilitation outcomes. The results indicated that incorporating neck muscles and head structures facilitated more biomechanically realistic outcome measures for guiding ACDF implant design. Moreover, our research findings indicated that the implant design with PEEK material preserved the neck angular motion and reduced disk stresses, while with Ti material, it led to decreased neck motion and increased disk stresses. These findings can guide surgeons in choosing implant materials and thus assist patients in enhancing postsurgery neck performance, shortening return-to-duty times, and reducing the need for secondary surgeries. In summary, our study contributes to theoretical knowledge and provides actionable guidance for advancing clinical practices in ACDF. Our future endeavors include evaluating current ACDF implant designs using alternate material properties and other novel geometric designs, in addition to investigating other factors such as wear rate, long-term osseointegration, and biocompatibility by employing a combination of computational simulations and experimental approaches to provide a comprehensive assessment.

ACKNOWLEDGMENTS

We would like to thank Dr Sudeesh Subramanian and Mr Gustavo Paulon for their helpful comments. This work was supported, in part, by the National Science Foundation (223910), the Department of Homeland Security (70RSAT21CB0000023), and the Texas Tech Neuroimaging Institute.

INDIVIDUAL AUTHOR CONTRIBUTION STATEMENT

H.B. contributed to conceptualizing and developing the model, performing the simulations, and writing the manuscript. S.K.C. contributed to conceptualization, study supervision, and manuscript editing and revision.

INSTITUTIONAL CLEARANCE

Not applicable.

FUNDING

This work was supported, in part, by the National Science Foundation (223910), the Department of Homeland Security (70RSAT21CB0000023), and the Texas Tech Neuroimaging Institute.

SUPPLEMENT SPONSORSHIP

This article appears as part of the supplement "Proceedings of the 2023 Military Health System Research Symposium," sponsored by Assistant Secretary of Defense for Health Affairs.

CONFLICT OF INTEREST STATEMENT

None declared.

DATA AVAILABILITY

The data supporting this study's findings are available on request from the corresponding author.

REFERENCES

1. Irvine D, Foster J, Newell D, Klukvin B: Prevalence of cervical spondylosis in a general practice. Lancet 1965; 285(7395): 1089–92. 10.1016/S0140-6736(65)92674-7
2. Moussa A, Tanzer M, Pasini D: Cervical fusion cage computationally optimized with porous architected titanium for minimized subsidence. J Mech Behav Biomed Mater 2018; 85(23): 134–51. 10.1016/j.jmbbm.2018.05.040
3. Byeon JH, Kim JW, Jeong HJ, et al: Degenerative changes of the spine in helicopter pilots. Ann Rehabil Med 2013; 37(5): 706–12. 10.5535/arm.2013.37.5.706
4. Tolga Aydoğ S, Türbedar E, Akin A, Doral MN: Cervical and lumbar spinal changes diagnosed in four-view radiographs of 732 military pilots. Aviat Space Environ Med 2004; 75(2): 154–7. 10.3357/ASEM.2472.2004
5. McCormick JR, Sama AJ, Schiller NC, Butler AJ, Donnally CJ: Cervical spondylotic myelopathy: a guide to diagnosis and management. J Am Board Fam Med 2020; 33(2): 303–13. 10.3122/jabfm.2020.02.190195
6. New PW, Cripps RA, Bonne Lee B: Global maps of non-traumatic spinal cord injury epidemiology: towards a living data repository. Spinal Cord 2014; 52(2): 97–109. 10.1038/sc.2012.165
7. Smith GW, Robinson RA: The treatment of certain cervical-spine disorders by anterior removal of the intervertebral disc and interbody fusion. J Bone Joint Surg Am 1958; 40(3): 607–24. 10.2106/00004623-195840030-00009
8. Cloward RB: The anterior approach for removal of ruptured cervical disks. J Neurosurg 1958; 15(6): 602–17. 10.3171/jns.1958.15.6.0602
9. Lin M, Paul R, Dhar UK, et al: A review of finite element modeling for anterior cervical discectomy and fusion. Asian Spine J 2023; 17(5): 949–63. 10.31616/asj.2022.0295
10. Huang H, Liu J, Wang L, Fan Y: A critical review on the biomechanical study of cervical interbody fusion cage. Med Nov Technol Devices 2021; 11(1): 1–38. 10.1016/j.medntd.2021.100070
11. Saifi C, Fein AW, Cazzulino A, et al: Trends in resource utilization and rate of cervical disc arthroplasty and anterior cervical discectomy and fusion throughout the United States from 2006 to 2013. Spine J 2018; 18(6): 1022–9. 10.1016/j.spinee.2017.10.072
12. Dmitriev AE, Cunningham BW, Hu N, Sell G, Vigna F, McAfee PC: Adjacent level intradiscal pressure and segmental kinematics following a cervical total disc arthroplasty: an: in vitro: human cadaveric model. Spine 2005; 30(10): 1165–72. 10.1097/01.brs.0000162441.23824.95
13. Tumialán LM, Ponton RP, Cooper AN, Gluf WM, Tomlin JM: Rate of return to military active duty after single and 2-level anterior cervical discectomy and fusion: a 4-year retrospective review. Neurosurgery 2019; 85(1): 96–104. 10.1093/neuros/nyy230
14. Panzer MB, Fice JB, Cronin DS: Cervical spine response in frontal crash. Med Eng Phys 2011; 33(9): 1147–59. 10.1016/j.medengphy.2011.05.004
15. Sun J, Wang Q, Cai D, et al: A lattice topology optimization of cervical interbody fusion cage and finite element comparison with ZK60 and Ti-6Al-4V cages. BMC Musculoskelet Disord 2021; 22(1): 1–14. 10.1186/s12891-020-03840-y
16. Maohua Lin RP, Shapiro SZ, Doulgeris J, O'Connor TE, Tsai C-T, Vrionis FD: Biomechanical study of cervical endplate removal on subsidence and migration in multilevel anterior cervical discectomy and fusion. Asian Spine J 2022; 16(5): 615–24. 10.31616/asj.2021.0424
17. Lehmann CL, Buchowski JM, Stoker GE, Riew KD: Neurologic recovery after anterior cervical discectomy and fusion. Global Spine J 2014; 4(1): 41–6. 10.1055/s-0033-1360723
18. Manickam PS, Roy S, Shetty GM: Biomechanical evaluation of a novel S-type, dynamic zero-profile cage design for anterior cervical discectomy and fusion with variations in bone graft shape: a finite element analysis. World Neurosurg 2021; 154(1): 199–214. 10.1016/j.wneu.2021.07.013
19. Liu J, Wang R, Wang H, et al: Biomechanical comparison of a new memory compression alloy plate versus traditional titanium plate for anterior cervical discectomy and fusion: a finite element analysis. Biomed Res Int 2020; 2020: 1–10. 10.1155/2020/5769293
20. Lin M, Shapiro SZ, Doulgeris J, Engeberg ED, Tsai C-T, Vrionis FD: Cage-screw and anterior plating combination reduces the risk of micromotion and subsidence in multilevel anterior cervical discectomy and fusion—a finite element study. Spine J 2021; 21(5): 874–82. 10.1016/j.spinee.2021.01.015
21. Kwon J-W, Bang S-H, Kwon Y-W, et al: Biomechanical comparison of the angle of inserted screws and the length of anterior cervical plate systems with allograft spacers. Clin Biomech 2020; 76(1): 1–7. 10.1016/j.clinbiomech.2020.105021
22. Gierczycka D, Rycman A, Cronin D: Importance of passive muscle, skin, and adipose tissue mechanical properties on head and neck response in rear impacts assessed with a finite element model. Traffic Inj Prev 2021; 22(5): 407–12. 10.1080/15389588.2021.1918685
23. Correia MA, McLachlin SD, Cronin DS: Vestibulocollic and cervicocollic muscle reflexes in a finite element neck model during multidirectional impacts. Ann Biomed Eng 2021; 49(7): 1645–56. 10.1007/s10439-021-02783-2
24. Eckersley CP, Nightingale RW, Luck JF, Bass CR: Effect of neck musculature on head kinematic response following blunt impact. *Proceedings of the IRCOBI* Antwerp, Belgium. 2017: 685–98.
25. Ito S, Ivancic PC, Pearson A, et al: Cervical intervertebral disc injury during simulated frontal impact. Eur Spine J 2005; 14(4): 356–65. 10.1007/s00586-004-0783-4
26. Noordhoek I, Koning MT, Jacobs WC, Vleggeert-Lankamp CL: Incidence and clinical relevance of cage subsidence in anterior cervical discectomy and fusion: a systematic review. Acta Neurochir 2018; 160(4): 873–80. 10.1007/s00701-018-3490-3
27. Qi Y, Lewis G: Influence of assigned material combination in a simulated total cervical disc replacement design on kinematics of a model of the full cervical spine: a finite element analysis study. Bio-Med Mater Eng 2016; 27(6): 633–46. 10.3233/BME-161614
28. Chen Y, Wang X, Lu X, et al: Comparison of titanium and polyetheretherketone (PEEK) cages in the surgical treatment of multilevel cervical spondylotic myelopathy: a prospective, randomized, control study with over 7-year follow-up. Eur Spine J 2013; 22(7): 1539–46. 10.1007/s00586-013-2772-y

29. Niu -C-C, Liao J-C, Chen W-J, Chen L-H: Outcomes of interbody fusion cages used in 1 and 2-levels anterior cervical discectomy and fusion: titanium cages versus polyetheretherketone (PEEK) cages. Clin Spine Surg 2010; 23(5): 310–6. 10.1097/bsd.0b013e3181af3a84
30. Seaman S, Kerezoudis P, Bydon M, Torner JC, Hitchon PW: Titanium vs. polyetheretherketone (PEEK) interbody fusion: meta-analysis and review of the literature. J Clin Neurosci 2017; 44(1): 23–9. 10.1016/j.jocn.2017.06.062
31. Manickam PS, Roy S: The biomechanical effects of S-type dynamic cage using Ti and PEEK for ACDF surgery on cervical spine varying loads. Int J Artif Organs 2021; 44(10): 748–55. 10.1177/03913988211039525
32. Bahreinizad H, Chowdhury SK, Paulon G, Wei L, Santos FZ: Development and validation of an MRI-derived head-neck finite element model. bioRxiv 2023; 1–30. 10.1101/2023.02.12.528203.
33. Deurenberg P, Weststrate JA, Seidell JC: Body mass index as a measure of body fatness: age- and sex-specific prediction formulas. Br J Nutr 1991; 65(2): 105–14. 10.1079/BJN19910073
34. Stober EJ, Seferis JC, Keenan JD: Characterization and exposure of polyetheretherketone (PEEK) to fluid environments. Polymer 1984; 25(12): 1845–52. 10.1016/0032-3861(84)90260-X
35. Zhang L, Yang KH, King AI: A proposed injury threshold for mild traumatic brain injury. J Biomech Eng 2004; 126(2): 226–36. 10.1115/1.1691446
36. Bradke BS, Miller TA, Everman B: Photoplethysmography behind the ear outperforms electrocardiogram for cardiovascular monitoring in dynamic environments. Sensors 2021; 21(13): 1–15. 10.3390/s21134543
37. Madison AM, Stewart A, Robinette A, Sous S, Yoganandan N, Chancey VC et al: Surgical Interventions for Cervical Intervertebral Disc Disease in U.S. Army Aviators: A Comprehensive Review and Identification of Knowledge Gaps. 1186076: Defense Technical Information Center, 2022.
38. Eckner JT, Oh YK, Joshi MS, Richardson JK, Ashton-Miller JA: Effect of neck muscle strength and anticipatory cervical muscle activation on the kinematic response of the head to impulsive loads. Am J Sports Med 2014; 42(3): 566–76. 10.1177/0363546513517869
39. Arts M, Torensma B, Wolfs J: Porous titanium cervical interbody fusion device in the treatment of degenerative cervical radiculopathy; 1-year results of a prospective controlled trial. Spine J 2020; 20(7): 1065–72. 10.1016/j.spinee.2020.03.008
40. Boughton OR, Ma S, Zhao S, et al: Measuring bone stiffness using spherical indentation. PLoS One 2018; 13(7): 1–18. 10.1371/journal.pone.0200475